Evolutionary stability of social commitment

Short title: Evolutionary stability of social commitment

Yuka Shirokawa [a, *], Masakazu Shimada [a], Nao Shimada [a], Satoshi Sawai [a, b]

[a] Graduate School of Arts and Sciences, University of Tokyo, Tokyo 153-8902, Japan;
[b] Research Center for Complex Systems Biology, University of Tokyo, Tokyo 153-8902, Japan;

[*] To whom correspondence should be addressed: Yuka Shirokawa (ORCID: 0000-0003-4825-7190) shirokawa.yuka@gmail.com

Abstract

The social amoeba *Dictyostelium discoideum* switches between the phase of solitary growth and social fruitification depending on nutrient availability. Under non-nutrient conditions, cells enter the social phase where they aggregate and differentiate to form fruiting bodies consisting of spores on top of non-viable altruistic stalk cells. Once cells aggregate, they complete fruiting body formation even with a renewed source of nutrients. This social commitment is puzzling because it deprives individual cells of the benefits of quickly resuming solitary growth. One idea posits that traits that facilitate premature dedifferentiation in response to nutrient recovery are somehow hindered from being selected in a social context. In this study, we studied the outcomes of premature dedifferentiation by forced refeeding. We show that when refed cells were allowed to resume sociality together with non-refed cells, besides some successfully becoming solitary outside of fruiting bodies, a large fraction was redirected to a sub-region of altruistic stalk regardless of their original cell fate. The lower cohesiveness of prestalk cells relative to prespore cells and comparably reduced cohesivity in refed cells was consistent with the redirection. Furthermore, application of a game theoretical model, which describes fruiting body formation among cells with differences in cell-cell association strategies, revealed a valley in the fitness landscape that prevents the invasion of mutants with the ability to dedifferentiate completely into a socially committed population. Our results provide a general scheme that naturally penalizes withdrawal from a society by evolving a specific division of labor such that less cohesive individuals become altruists.

Significance Statement

Evolution of unicellular to multicellular organisms must resolve conflicts of reproductive interests between individual cells and the group. In the social amoeba *Dictyostelium*, a transition from a solitary to multicellular group occurs under starvation. Once cells commit themselves to multicellular organization, the process continues even when shifting to an environment that favors solitary growth. Our study revealed that cells forced to partially revert to a de-committed state take an altruistic role through interaction with socially committed cells. The de-committed cells exhibited reduced cohesivity and were sorted out to altruistic positions in morphogenesis. This inevitably penalizes 'selfish' cells that revert to solitary growth too quickly. Our results explain group-level behaviors that is apparently difficult to understand from an individual-level fitness.

Key words: Cooperation; physiological irreversibility; valley of fitness landscape; division of labor; developmental stability; multicellularity

Introduction

Continued social interactions are fundamental to make cooperation fruitful for group members. However, the evolution of sociality is often faced with selection pressures that potentially lead to their collapse. Cheating that exploits the benefit of cooperation at the cost of others is a well-studied case of such risks. Nature has found ways to reduce the deleterious effects of cheating by making use of interactions among kin (1) and policing that suppress individual proliferation (2). In microbial cooperation (3), spatial interactions that keep the cooperator cells at close distances, such as spatial genetic drift in expanding colonies (4, 5) and kin recognition using cell-surface proteins (6, 7) play pivotal roles in reducing the advantage of cheating mutants. Besides cheating, sociality is also vulnerable to environmental changes that raise fitness of a cell as a solitary individual rather than as a social group member. Indeed, evolutionary loss of social behavior has been experimentally demonstrated in myxobacteria under conditions that impede their social interaction while favoring solitary reproduction (8). Phylogenetic and behavioral analyses have also shown that the evolutionary loss of social behavior appears to be a common phenomenon across taxa from insects to unicellular organisms (9–11). Social behavior exemplified by a high degree of division of labor and reproductive skew, in general, is thought to have crossed a 'point of no return' (12, 13) back to a solitary lifestyle due to its high complexity. The stabilization of cooperation against adverse evolutionary pressures is thought to be the key driving force that increases social complexity (14, 15).

How sociality is precluded from reverting to a free-living behavior is especially non-trivial in social groups consisting of individual cells that can survive on their own. One explanation is that social traits act disadvantageously for unicellular growth. For example, in the experimental evolution of fission yeast, high rates of apoptosis evolve because they promote snowflake-like sparse chains of clustered cells, which increases access to more nutrients and space. Since apoptosis is inevitably disadvantageous for solitary proliferation (14, 16), the antagonizing effect should facilitate the maintenance of multicellular traits (14, 15). However, such a trade-off may be limited to cases where individual cells can immediately escape the group, as is true in the case of the yeast snowflakes. In more elaborate multicellular groups, evolutionary transitions must occur in steps. Under selection pressure for solitary proliferation, myxobacteria exhibit intermediate social behaviors such as reduced frequency of sporulation and collective motility (8), hinting at the importance of intermediate phenotypes in the evolutionary transition (17). Given that sociality is a multifactorial trait that is regulated and constrained by a large number of genes, even in simple multicellularity (18), loss of sociality almost inevitably proceeds through a transition stage where a newly emerging lineage

106 exhibits the intermediate phenotype, meaning that it still interacts with the majority of other
107 socially committed cells within the multicellular group. In this situation, evolutionary
108 reversion may be prevented by a mechanism to suppress the proliferation of cells with the
109 intermediate phenotypes. However, when proliferation as free-living cells outweighs the
110 benefit of cooperation, social lineages should not be able to acquire a new costly
111 countermeasure. It is still possible that the preexisting social behavior itself comes with rather
112 unexpected bonus of acting inhibitory to reversion to a solitary lifestyle. If the intermediate
113 phenotype is recognized as 'nonself' from other social members, a defensive function that
114 social groups are equipped with can potentially harm them due to their incomplete target
115 specificity. For example, social microbes evolve traits that suppress the sporulation of
116 cheaters (19, 20). Although such suppression is thought to result from a mechanism that
117 adapts to combat competitors, how specific it is to a certain genotype is poorly explored. In
118 other examples, bacteriocins that suppress competitors are expected to spite cells that are
119 sensitive to the signal in an indiscriminatory manner (21). Given that such elimination of
120 'nonself' are common and fundamental defense strategies in both unicellular and multicellular
121 organisms (22), what may underlie many of the suppressive behaviors are some basic
122 mechanisms that exclude deviators from the original members, which would inevitably
123 suppress the intermediate phenotypes. Taken together, how the intermediate phenotypes
124 between a social and solitary state interact with the original social members is critical in
125 understanding the maintenance of social behaviors.
126 The social amoeba *Dictyostelium discoideum* is a soil-living eukaryote with
127 facultative sociality under non-nutrient conditions (23, 24). The cells grow and divide in the
128 presence of nutrient sources such as bacteria and fungi, however, when starved, they stop
129 foraging and aggregate to form a multicellular slug that culminates in a fruiting body composed
130 of differentiated spores and stalk cells. *Dictyostelium* has served as a model microorganism
131 to study cellular cooperation (25), especially since vacuolation and death of stalk cells that
132 support the spores (23, 24) can be viewed as an altruistic behavior. Interestingly, after 4 to 6
133 hours of starvation onward, cells become engaged in the differentiation process (26), and will
134 no longer quickly revert back to the growth phase even with renewed nutrient supply (27).
135 Instead, cells continue with the formation of fruiting bodies within 24 hours. The inability of
136 differentiating cells to switch back to the state of solitary amoeba (hereafter referred to as social
137 commitment) is dependent on the multicellular context. When cells that are mechanically
138 dissociated are replenished with nutrients, they dedifferentiate and revert to solitary growth
139 (26–28). Thus, unless differentiating cells are forced to separate and feed, the only way by
140 which cells can return to the solitary state is to first mature into encapsulated spores and then

141 to germinate, a long process that takes a few days. The evolutionary benefit of the social
142 commitment is puzzling, especially given that the social amoeba colonizes sites with
143 fluctuations in the nutrient environment, such as a frequent supply of rich dung or leaf mold
144 (29), which favor quick reversion to solitary proliferation. Existence of a phagocytic cell-type
145 that serves to remove intruding bacteria (30) suggests that it is not unusual for cells within a
146 slug to be exposed to nutrients. Given the fact that these cells are very small in number, it is
147 not hard to imagine situations where they are outnumbered and thus permitting strong invasive
148 perturbation similar to the idealized refeeding experiments in this work. To understand the
149 multicellular basis that maintains the social commitment in *Dictyostelium*, we studied the
150 outcome of cells that revert to a partially de-committed state while still in association with
151 socially committed cells. In our experiments, cells were forced to take the dedifferentiation
152 path by short-term refeeding, and their fates when mixed with socially committed cells were
153 traced by live-cell imaging. Based on the observation, a theoretical model was constructed
154 and analyzed to predict the evolutionary stability of the social commitment.
155
156
157 # Results
158 **Forced refeeding experiments**
159 Mechanically dissociated cells re-plated on agar without nutrients are known to rapidly
160 reaggregate and recapitulate the respective developmental stages within a few hours (31). We
161 exploited this unique property to investigate the interactions between socially committed and
162 de-committed cells. For partially de-committed cells, dissociated cells from the slug stage
163 were fed with bacteria *Escherichia coli* B/r for 3 or 5 h (hereafter referred to as RF3 and RF5
164 cells, respectively), then nutrients were removed again. The refed cells were then allowed to
165 reaggregate with cells that were not refed (NF cells, socially committed cells) (Fig. 1*A*). Thus,
166 this treatment mimics a situation that a rare cell makes a slug with socially committed cells, and
167 dedifferentiates due to engulfing bacteria within the slime sheath of the slug, where the bacteria
168 remained for 3 to 5 h before the terminal differentiation (approximately 18 to 23 h after
169 starvation). To track the cells, a strain harboring the prestalk (ecmAO-RFP) and prespore
170 (pspA-GFP) marker genes were used. Owing to the relatively long time (> 4–5 h) required
171 for the preexisting fluorescent proteins degrade (32), the fluorescence was used as identification
172 of their original cell fate. The parental strain without the fluorescent marker genes was used
173 for the negative identification of NF cells. The mixture of cells co-aggregated and jointly
174 formed a tight mound after 1.5–2 h (Fig. S1, Movies S1 and S2). In the mixture of NF cells
175 with and without the cell-type reporter (NF+NF), prestalk cells were found in the peripheral

176 region of the aggregate, while prespore cells were more uniformly distributed (Fig. 1*B*: NF+NF)
177 in line with the previously described sorting pattern (33). In contrast, in the mixed aggregates
178 of RF and NF cells, RF cells (fluorescent cells) were positioned at the periphery regardless of
179 the original cell type (Fig. 1*B*: RF3/5+NF), while NF cells (non-fluorescent cells) were more
180 abundant in the center of the aggregate. The refed treatment significantly affected cell
181 positioning, and the difference in prespore positioning between the control and the refed
182 condition was evident (Fig. 1*C*: overall model: GLM and analysis of deviance, cell fate: $F_{1,186}$
183 $= 228.661$, $P < 0.0001$, treatments: $F_{2,184} = 56.447$, $P < 0.0001$, prespore cells in NF+NF versus
184 RF5+NF: *t*-test, d.f. = 36.687, t = -7.606, adjusted $P < 0.0001$).
185 In the swap control, we observed a reciprocal pattern of fluorescent cells in the center
186 and non-fluorescent cells in the periphery (Fig. S2*A*, RF(Fl-)+NF(Fl+)), indicating that
187 expression of the marker genes itself did not affect the sorting pattern. RF cells were still fully
188 capable of developing on their own, forming a tipped mound of normal morphology with timing
189 indistinguishable from the NF cells (Fig. S2*B*). These results demonstrate that segregation
190 was not due to the innate inability of RF cells to develop, but rather a relative behavior when
191 in association with the NF cells. Cells dissociated and shaken without refeeding did not
192 segregate from the freshly dissociated cells (Fig. S2*C*, RF(No-nutrient)+NF). Furthermore,
193 refeeding with liquid growth medium had the same effect as refeeding with bacteria (Fig. S2*C*,
194 RF(growth medium)+NF). These results indicate that the unique sorting pattern was not
195 merely due to mechanical interruption but also required nutrient replenishment. Quantitative
196 real-time polymerase chain reaction (real-time PCR) analysis of the dissociated cells in
197 suspension with or without nutrients (Table S1, see *SI* Methods) showed distinct patterns of
198 gene regulation compared to unperturbed samples whose changes were relatively small (Fig.
199 1*D*, 'No-dissociation'). Dissociated cells exhibited reduced expression of cell-type
200 differentiation marker genes (Fig. 1*D*, *pspA*, *ecmA*), indicating that dissociated cells were
201 partially dedifferentiating regardless of the presence or absence of nutrients (bootstrap test,
202 adjusted $P > 0.05$, Fig. 1*D*). Whereas genes encoding the main adhesion molecules (34) (*cadA*,
203 *csaA*, and *tgrC1*) did not show nutrient-specific changes, *carA*, *acaA*, *pdsA,* and *dscA* genes
204 (Fig. 1*D*) showed contrasting activity of being reduced by refeeding and induced in non-nutrient
205 buffer (GLM and analysis of deviance, 'No-nutrient' versus 'Bacteria': adjusted $P < 0.05$, 'No-
206 nutrient' versus 'Growth medium': adjusted $P < 0.01$, Fig. 1*D*). *CarA*, *acaA*, and *pdsA* are
207 essential for the cAMP relay during cell aggregation, and *carA* is also required for chemotaxis
208 to the relayed cAMP. *dscA* (discoidin I) is a GRGD (Gly-Arg-Gly-Asp) containing lectin
209 implicated in the cell-substratum adhesion of cell streams during aggregation (35, 36).

210 Given that the refed cells show markedly reduced expression of the re-aggregation
211 genes, they are likely to fall behind in joining the cell clusters compared to the non-refed cells
212 by delayed chemotaxis. A close observation of cell reaggregation, however, revealed that
213 refed cells often appear well mixed in the aggregate initially and then sorted out afterwards
214 (Movie S2). A recent work suggested a concerted sorting mechanism of a tip-forming prestalk
215 subtype by competition between chemotaxis and cell-cell contact-based collective movement
216 during mound regeneration (37). In the present case, however, the refed cells sorted to the
217 periphery and then to the base of the mound instead of the apical tip (Fig. S3*A*). Furthermore,
218 the refed cells did not exhibit collective movement, but rather appeared to be sorted out
219 gradually without directed migration (Movie S2). These observations point to an alternative
220 mechanism of cell segregation based on differential adhesion (38), where cell-type that position
221 themselves in the peripheral region of a cell mass should be less cohesive than those positioned
222 in the inner region. We tested the ability of RF cells to associate with aggregates using a
223 cohesion assay (39). Briefly, mechanically dissociated cells were suspended in the phosphate
224 buffer and shaken gently to facilitate cell agglutination by random collisions for 1.5, 3, and 5 h,
225 and the number of single unattached cells was quantified (Fig. 1*E* left, see SI Methods). For
226 RF conditions, the assay was performed under the continued presence of nutrients to avoid the
227 chemotaxis effect by cAMP. We found that cells in the bacterial suspension or liquid growth
228 medium were less cohesive (Fig. 1*E* left, 'Bacteria', 'Growth medium') than those in the
229 phosphate buffer (Fig. 1*E* left: GLM and analysis of deviance, Buffer 5 h versus Bacteria 5 h:
230 deviance = 424.93, d. f. = (1, 4), adjusted $P < 0.0001$, Buffer 5 h versus Growth medium:
231 deviance = 748.4, d. f. = (1, 4), adjusted $P < 0.0001$). These results are consistent with an
232 earlier finding indicating a reduction in cell-cell cohesion during dedifferentiation (40). In
233 addition, we found that the prespore cells constituted 55% of the unattached cells within the
234 phosphate buffer (Fig. 1*E* right, Buffer 5h, the gray bar), which deviated markedly from the
235 prespore percentage (82%) when most cells were in a single state (Fig. 1*E* right, Buffer+EDTA,
236 the white bar: GLM and analysis of deviance, Buffer+EDTA versus Buffer 5 h: deviance =
237 9.438, d.f. = (1, 4), adjusted $P < 0.0001$). The occurrence of unattached prespore cells in the
238 presence of bacteria (Fig. 1*E* right, shaded bars 1.5, 3, and 5h) was comparable to that of the
239 non-adhesive control, thus the refed prespore cells tended to be more solitary state
240 (Buffer+EDTA versus Bacteria 5 h: deviance = 13.964, d.f. = (1, 4), adjusted $P = 0.572$). Our
241 results indicate that prestalk cells are less cohesive than the prespore cells in line with earlier
242 literature (41). The lower cohesiveness of prestalk cells relative to prespore cells (Fig. 1*E*
243 right) and comparably reduced cell-cell cohesivity in refed cells (Fig. 1*E* left) are consistent
244 with the peripheral positioning (Figs. 1*B* and *C*) of these cells.

245 Positional bias was also evident during the culmination. The fruiting body of *D.*
246 *discoideum* consists of a spore mass held aloft by a stalk. In addition to the main stalk, stalk
247 cells constitute three other distinct terminal cell types: The upper and the lower cups and the
248 basal disc (Fig. 2*A*) (24). 4–6 h after plating, the cell mass elongated into a finger-like form
249 with a prespore cell mass between the two prestalk regions that later became the upper and the
250 lower cups, respectively (Figs. 2*B* and 2*C*, Fig. S3*B*, Movie S3), and the normal patterning was
251 observed in NF cell populations (Fig. 2*B*: NF+NF). Accordingly, the positional frequency of
252 prespore and prestalk cells along the anterior-posterior axis was strongly anti-correlated (Fig.
253 2*B* NF+NF, GLM and analysis of deviance, slope = -2.03 ± 0.26, $F_{1,1198} = 59.21$, $P < 0.0001$).
254 In contrast, in RF+NF populations, RF cells were abundant in the lower region (Fig. 2*B*, Fig.
255 S3*B*, Movie S4: RF3+NF, RF5+NF). Consequently, the positional frequency of prespore and
256 prestalk cells was positively correlated (Fig. 2*B,* GLM and analysis of deviance, RF3+NF: slope
257 = 4.53 ± 0.25, $F_{1,998} = 356.89$, $P < 0.0001$, RF5+NF: slope = 3.70 ± 0.31, $F_{1,648} = 152.38$, $P <$
258 0.0001). Later, these RF cells formed the future lower cup and the basal disc but were almost
259 completely excluded from the upper cup and the main stalk (Fig. 2*C*, RF3+NF). A consistent
260 pattern was observed in the marker swap controls (Fig. 2*C*, RF3(Fl-):NF(Fl+) = 85:15,
261 RF3(Fl+):NF(Fl-) = 70:30) indicating that the sorting pattern was not due to the choice of
262 fluorescent marker strains. Interestingly, there appeared to be a gradient-like sorting
263 preference in the posterior (lower) to anterior (upper) axis of the culminant. In our standard
264 condition where RF cells were the minority, RF cells of both the prespore- and prestalk-origin
265 segregated to the lower prestalk region (Fig. 2*C*, RF3+NF). When RF cells were the majority,
266 the refed prespore and prestalk cells were positioned according to their original cell fate.
267 However, there was still a positional bias within each domain: RF cells of prespore-origin were
268 found in the lower portion of the spore mass, and those of prestalk-origin occupied a lower
269 portion of the upper cup in addition to the lower cup (Fig. 2*C*, RF3(Fl+):NF(Fl-) = 70:30).
270 In the final hours of terminal differentiation (8 to 10 h after plating), the ectopic
271 positioning of refed cells was most notable in the basal disc region, which consists mainly of
272 secreted cellulose and vacuolating non-viable cells (42, 43). In the controls ('No-dissociation',
273 NF+NF), the basal disc was occupied by cells of prestalk-origin (Figs. 2*D* and *E*: 'No-
274 dissociation', NF+NF) as expected (44). In contrast, RF+NF (Figs. 2*D* and *E*: RF3+NF,
275 RF5+NF), RF cells of both prestalk and prespore origins were found intermingled with non-
276 fluorescent NF cells at the basal disc (Figs. 2*D* and *E*, overall model: GLM and analysis of
277 deviance, $F_{3,94} = 25.008$, $P < 0.0001$, control versus Rf5: *t*-test, d.f. = 18.888, t = -12.292,
278 adjusted $P < 0.0001$). In addition, cells scattered around the base (45) were amoeboid and
279 showed random movement (Movie S5), indicating that the cells escaped cell death as stalks.

In the non-feeding controls, these scattered cells on the agar surface were of prestalk origin (Figs. 2*F* and *G*: 'No-dissociation', NF+NF), whereas in the RF+NF populations (Figs. 2*F* and *G*: RF3+NF, RF5+NF), RF cells of both prespore and prestalk origins were found scattered around the basal disc (Figs. 2*F* and *G*: overall model: GLM and analysis of deviance, $F_{3,86} = 41.432$, $P < 0.0001$, NF+NF versus RF5+NF: *t*-test, d.f. = 23.099 , t = -21.81, adjusted $P < 0.0001$). The results (Figs. 2*F* and *G,* Movie S5) indicate that the final survivors at the terminal phase included some solitary cells (amoeba) in addition to social cells (spores). In the terminal differentiation, RF cells in the RF+NF populations were more allocated to the solitary amoeboid cells than NF cells (Fig. S4).

The growth cost of the social commitment

Our refeeding experiments indicate that *Dictyostelim* cells that dedifferentiate precociously are penalized by being assigned a role of non-viable stalk (Figs. 1 and 2). This observation is interesting from an evolutionary point of view as it may reduce competitive disadvantages of socially committed cells under nutrient-rich environments. Given this, we went on to investigate a basic question of how the social commitment imposes individual cells growth costs. If cells experience nutrient recovery at the slug stage ($s = 18$h, Fig. 3*A*), socially committed cells should proceed to the later stages of development: Only rare solitary cells would be able to grow (46, 47). Therefore, the socially committed cells would bear two types of growth costs: Growth delay incurred by fruiting body formation (d) and lag time for spore germination (λ) (Fig. 3*A*). On the other hand, without commitment, cells would revert to a solitary state immediately after refeeding (Fig. 3*A*). For quantification of the growth cost, cells were released from the commitment by mechanical dissociation. After 30h-incubation from the slug stage (Fig. 3*A*: d), amoeboid cells and spores were harvested, and cell growth was measured within the growth medium (Fig. 3*A*, 'Growth assay'). This result shows that despite nutrient recovery, cell growth was delayed for approximately 9 h if cells were not mechanically dissociated (Fig. 3*B*, [Estimated lag time λ, 'Refed & Dissociation': 15.24 ± 4.27 h, 'Refed & No-dissociation': 23.97 ± 4.35 h, 'Continuous starvation': 36.17 ± 4.03 h], [Estimated growth rate: 'Refed & Dissociation': 0.067 ± 0.012, 'Refed & No-dissociation': 0.064 ± 0.012, 'Continuous starvation': 0.057 ± 0.009]). The significant growth delay (Fig. 3*B*, 'Refed & No-dissociation' versus 'Refed & Dissociation': GLM and analysis of deviance, $F_{1,21} = 12.175$, $P < 0.003$) highlights the cost for individual cells of remaining in the social group under nutrient-rich environments.

315 **Model analysis for evolutionary maintenance of the social commitment**

316 If the non-committed strain is rewarded by such a growth advantage (Fig. 3), how stable is
317 social commitment against adverse evolutionary pressures? To investigate how well the cell-
318 fate reallocation (Figs. 1 and 2) could help maintain sociality, we analyze whether a rare mutant
319 cell that reverts to the solitary state could invade a wild-type population with the framework of
320 adaptive dynamics (48, 49). We considered a sufficiently large population of haploid and
321 asexually reproducing cells which are exposed to nutrient recovery at each slug stage. The
322 evolutionary trait is a degree of association with other cells, x $(0 \leq x \leq 1)$ (Table S2). Cells
323 with any of the traits normally commit to the development and differentiation, and then express
324 the trait x at the slug stage, with both cell fate and fitness decided according to x. A wild-
325 type cell has the trait $x = x_{wt}$, where its default value is $x_{wt} = 1$ indicating full social
326 commission. According to the value of x, a single cell simultaneously has probabilities to be
327 a spore, stalk, and solitary cell. The probabilities are equivalent to the cell fate ratios in the
328 clonal population with the trait x. The cell fate ratios at the initial stage of the evolution ($x =$
329 1) are designated as $SP_{initial} = 0.6$, $ST_{initial} = 0.2$, and $Sol_{initial} = 0.2$, respectively (for
330 suitability of the parameters see, Fig. S5).

331 We consider that invasion of a rare mutant cell with the trait $x' = x_{wt} + \varepsilon$, ($\varepsilon$ is a
332 sufficiently small negative value), and the mutant evolves a reduced level of cell-cell
333 association, $x' < x_{wt}$. The rare mutant cell makes a chimera slug with the wild-type cells,
334 and expresses the trait x' within the slug and reverts to a solitary state. We assume that the
335 cell-cell association level x controls most of cohesion proteins as a 'master regulator', i.e.,
336 $x = 1$ indicates full social commission, and $x = 0$ is a solitary state where cohesion proteins
337 are completely degradated (Fig. 4*A*). According to previous study and our experimental
338 results (Fig. 1*E*) (41), cohesion of each cell fate is assumed to be distinctively different, and the
339 highest is prespore, followed by in the order of prestalk, solitary cell (hereafter the allocation is
340 referred to as 'canonical allocation'). When a cell has a reduced trait value ($x < 1$), the trait
341 expression may induce cohesion degradation at the slug stage as the conceptual illustration of
342 distribution shifts (Fig. 4*A*). For example, the prespore cell after the trait expression will
343 exhibit reduced cohesion similar to an original prestalk or solitary cell. From our refed
344 experiments (Figs. 1 and 2), a cell is assumed to play a cell fate role as determined by its own
345 cohesivity, rather than its original fate role. Thus, given the order of cohesion (Fig. 1*E*) (41),
346 a cell changes a role via evolution of reduced x in the order of prespore, prestalk, and solitary
347 cell (Fig. 4*B*). With these evolutionary steps being described by the following differential
348 equations:

$$\frac{dP(SP|x)}{dx} = k_1 P(SP|x),$$

$$\frac{dP(ST|x)}{dx} = -k_1 P(SP|x) + k_2 P(ST|x), \quad [1]$$

$$\frac{dP(Sol|x)}{dx} = -k_2 P(ST|x),$$

where $P(Z|x)$ is the probability of a cell with the trait x taking fate Z (SP: Spore, ST: Stalk, Sol: Solitary cell). k_1, and k_2 are the rates of cell fate transition ($k_1 > 0$, $k_2 > 0$). If $k_1 \gg k_2$, decrement of the spore probability is quickly but that of stalk probability is slow in the evolution (Eq. **1,** Fig. 4*B*). On the other hand, if $k_1 \ll k_2$, vice versa. Our refed experiments (Fig. 2) support the assumption $k_1 \gg k_2$, because we observed a much smaller number of RF cells in prespore region of early fruiting bodies (quick $P(SP|x)$ decrement) but abundant RF cells in the stalk region (lower cup and basal disc) (slow $P(ST|x)$ decrement). We could select default values as $k_1 = 14.6$ and $k_2 = 6.3$, when evaluating cell fate transition through shifts in the cohesion distribution following evolution of *x* (see, SI text). The equation (Eq. **1**) is solved under the initial value at $x = 1$ (prespore: $SP_{initial}$, prestalk: $ST_{initial}$, solitary: $Sol_{initial}$). Both the wild-type and mutant cells follow Eq. **1**.

Invasion fitness of the mutant cell is

$$W(x'; x_{wt}) = f(x'; x_{wt}) - f(x_{wt}; x_{wt}), \quad [2]$$

where, $f(x'; x_{wt})$ is survival probability of the mutant when the mutant interacts with the wild-type cell, and $f(x_{wt}; x_{wt})$ is that of the wild-type cell that interacts with other wild-type cell. Because the mutant is rare, interaction between mutant cells is ignored. Both $f(x'; x_{wt})$ and $f(x_{wt}; x_{wt})$ are defined as the sum of the probabilities of becoming a spore (social fitness) and a solitary amoeboid cell (solitary fitness) as follows,

$$f(x) = P(SP|x) + g\, P(Sol|x), \quad [3]$$

where, g represents the additional weight of solitary fitness as defined by nutrient availability. Thus, for simplicity, amounts of nutrients directly contribute the solitary fitness. Although the equation Eq. **3** simply describes the survival probability as a result of resource allocation between solitary and social life, stalk differentiation costs survival probability because $P(SP|x) + P(ST|x) + P(Sol|x) = 1$. We also consider another formulation that assumes the spore success explicitly depended on altruistic stalk investment, but the fitness plot (Fig. S6) shows fundamentally the same result as the formulation for the resource allocation (Eq. **3**).

The invasion fitness when the mutant interacts with the wild-type cell with $x_{wt} = 1$ (Fig. 4*C*) showed a fitness valley under intermediate nutrient-rich condition ($g = 1$), owing to

381 the transient increase in the stalk fate probability during the evolution. In the starved condition
382 ($g = 0$), the mutant is always disadvantageous, while in the nutrient-rich condition ($g = 10$)
383 the mutant rapidly evolves (Fig. 4*C*). Ecology-evolution-environment diagram (49) in Fig.
384 4*D* shows evolution under various environmental conditions and indicates that the evolutionary
385 equilibrium is $x = 0$ or $x = 1$ depending on the starting point of the evolution. The point
386 where the selection gradient vanishes, i.e. 'evolutionarily singular' (48, 49) is denoted as x^*.
387 The singular point x^* is in the 'bottom' of the valley (evolutionary repellor) (Fig. 4*D,*
388 'Canonical allocation'), and neither an evolutionarily stable strategy (ESS) (50) nor
389 convergence stable (48, 51) when evaluated under our assumed condition ($k_1 \gg k_2$) (for detail,
390 see SI text and Fig. S7). Thus, the model predicts that once the wild-type cells acquire
391 complete social commitment ($x = 1$), mutant invasion is blocked under a wide range of
392 intermediate nutrient-rich conditions.

393 The fitness valley (Figs. 4*C, D*) was caused by a direct consequence of division of
394 labor that assigns each cell fate with a varying degree of cell-cell cohesion in the order of
395 prespore > prestalk > solitary cell (canonical allocation). If the social amoeba were to
396 have an alternative type of allocation rule: With cohesion order of prestalk > prespore >
397 solitary cell (reverse allocation), and with prespore = prestalk > solitary cell (random
398 allocation), these systems did not prevent invasion of the solitary reversion mutant (Fig. 4*D*).
399 In the reverse allocation system, an evolutionary singular point x^* is partially solitary state
400 (Fig. 4*D*, 'Reverse allocation') and is ESS and convergence stable under our assumed condition
401 ($k_1 \gg k_2$) (see SI text). The singular point x^* is found under starved conditions, where cells
402 become more 'selfish' and a fruiting body is slightly vulnerable than that of the complete social
403 commitment: Cells differentiate into more spores but less stalk cells. Under nutrient-rich
404 conditions, complete solitary mutant ($x = 0$) evolved (Fig. 4*D*). In the random allocation
405 system, there is no singular point (see SI text), and the equilibrium is $x = 1$ under starvation
406 conditions, and $x = 0$ under nutrient-rich conditions (Fig. 4*D*, 'Random allocation'). Taken
407 together, only the canonical allocation system can protect the social commitment under
408 nutrient-rich conditions.

409 Finally, to understand the range of the social defense, invasion of a cheating mutant
410 is investigated in addition to the solitary reversion mutant. We consider a rare cheating mutant
411 cell that has higher probability to be a spore than the wild-type cell within a chimera. An
412 evolutionary trait i denotes additional spore investment at the slug stage, thus the initial cell
413 fate probabilities for prespore, prestalk, and solitary cells, are $SP_{initial} + i$, $ST_{initial} - i$, and
414 $Sol_{initial}$, respectively. The trait of the wild-type cell is $i = i_{wt}$ where $i_{wt} = 0$ is the
415 default value. The trait of the cheating mutant is $i = i' = i_{wt} + \theta$, (θ is a sufficiently small

416 positive value). Especially, we focused a prolonged development time from the slug stage: In
417 the social amoeba, in dark and unbuffered conditions, cells suspend its development as a
418 migrating slug for a few days, which is believed to be a trait associated with finding a suitable
419 place for spore dispersal (24). The migrating slug induces a series of changes in cell fates
420 closely resembling those associated with the canonical allocation system: There is a sub-
421 population of prestalk cells left behind in the tail of the slugs (46), which are compensated by
422 trans-differentiation of prespore cells to prestalk cells (52). The time t represents the
423 prolonged development time from the slug stage ($t = 0$), and $t = 1$ indicates the maximum
424 migration time. Cell fate transition over development time is described as differential
425 equations including the derivative with respect to time t (Eq. **S18-S20** in SI text), which are
426 solved with the initial condition at $t = 0$ (prespore: $P_0(SP) = SP_{initial} + i$, prestalk:
427 $P_0(ST) = ST_{initial} - i$, solitary: $P_0(Sol) = Sol_{initial}$). The invasion fitness of the cheating
428 mutant $W(i'; i_{wt})$ is the sum of the probabilities of becoming a spore and a solitary cell (Eq.
429 **S22**, Eq. **S23** in SI text). The selection gradient (Eq. **S24** in SI text) is constant with respect
430 to i, and we found the condition that the cheating mutant evolves (red lines in Fig. 5, Eq. **S25-**
431 **S27** in SI text). The model shows that the evolution of the cheating mutant is suppressed
432 under nutrient-rich conditions in the canonical allocation system, while in the reverse allocation
433 system the evolution is suppressed under starved conditions and enforced under nutrient-rich
434 conditions. In random allocation, cheating always evolves (Fig. 5). Thus, if the social
435 amoeba experiences only starved conditions, the reverse allocation system is suitable; however,
436 if nutrient-rich conditions, the canonical allocation system will demonstrate the comprehensive
437 defense capacity.
438
439

440 # Discussion

441 Maintenance of cooperation is inextricably linked to the choice of social members to be
442 dispersed from a society (53). We show the choice of the leavers can canalize 'point of no
443 return' in the social evolution (12, 13). In *Dictyostelium*, our results suggest a mechanism that
444 employs the division of labor in which cells with a less cohesive propensity become altruists.
445 The dedifferentiating *Dictyostelium* cells take a prestalk-like cell state through interaction with
446 differentiating cells (Figs. 1 and 2); thus, the system penalizes precocious solitary reversion
447 (Fig. 4). Unlike policing, which entails inescapable costs in general (2), in the present scheme,
448 penalization occurs naturally through fruiting body formation and the social amoeba seems not
449 to pay explicit costs.

450 Furthermore, our model (Fig. 5) showed that the social system can also effectively
451 reduce the advantage of cheating mutants, which is consistent with earlier experimental
452 observations using natural isolates that suggest that cell fate conversion in slug migration may
453 suppress cheating (54). From these results, it is tempting to speculate that the cooperative
454 system in the social amoeba could have first acquired fate allocation that is designed to suppress
455 cheating, and this in turn penalized solitary reversion as a byproduct. Given that the
456 dedifferentiation process is regulated by several thousand genes (28, 55), the presence of the
457 fitness valley (Figs. 4*C* and *D*) acts as a strong resistance to the social commitment to break
458 down. Furthermore, for microbes with large clonal populations, the chance of crossing the
459 fitness valley through genetic drift is slim (56) without additional mechanisms (57). Even if
460 the social amoeba crossed the valley, the evolutionary progression may be too slow to manifest
461 itself, since the dedifferentiation process is known to be robust to genetic perturbation (55).
462 The limited applicability of our model is that we did not consider homeostatic regulation of cell
463 fate proportions in the social amoeba (27). Our experimental observations showed that when
464 refed cells were in the majority (70%~ of the population), these cells tended to follow their
465 original cell fate developing fruiting bodies of normal morphology (Fig. 2*C*). Thus, the
466 penalization for the solitary reversion seems to be effective in restricted conditions where the
467 mutant is in the minority (~15% of the population). The frequency-dependency may buffer
468 cells from effects of the selection. Future experimental evolution studies should clarify the
469 actual evolutionary process given their genetic background and developmental processes.
470 How the social commitment of *Dictyostelium* is evolutionarily maintained has been
471 a long-standing question ever since the observation was first reported (27). Our experimental
472 results suggest an interesting cellular dynamics-based mechanism as to how this is implemented.
473 The initial prestalk-like positioning of refed cells to the mound periphery (Fig. 1*B*) can be
474 explained based on the mechanism of cell segregation (38) by differential adhesion of non-
475 refed cells and refed cells. Consistent with this notion, the low cohesiveness of refed cells
476 comparable to that observed in the prestalk cells was confirmed under our experimental
477 conditions (Fig. 1*E*). Later, the refed cells were positioned at the base of the mound (Fig.
478 S3*A*), which then formed the lower cup (Fig. 2*B*) and the basal disc (Fig. 2*D*). The basal disc
479 and lower cup are well-known terminal states of prestalk cells (44, 58), however, how cells are
480 positioned at these locations is not well understood. The localization of refed cells is distinct
481 from that of the primary stalk cells but similar to that of the 'anterior-like cells' (58–61) – a
482 small percentage of poorly characterized prestalk subtype that constitutes the basal disc, the
483 lower cup and the upper cup. The lack of refed cells from the upper cup makes it distinct from
484 the anterior-like cells. This, as well as its absence from the main stalk, may be related to

485 reduced sensitivity to cAMP due to the decreased *carA* gene expression in the refed cells (Fig.
486 1*D*), as low sensitivity to cAMP facilitates re-differentiation of prespore cells to lower cup cells
487 and inhibits prestalk cells positioning to the upper cup (62).
488 Cooperation is a fundamental force that leads to the emergence of collective-level
489 selection units (63, 64). Paradoxically, the fact that individuals are allowed to choose a
490 solitary strategy among other options, such as to cooperate or to cheat, can in turn maintain
491 cooperation by reducing cheating interest (65). In addition, the presence of cells ungrouped
492 can compensate cost of cooperation (66), and facilitate coexistence of diverse social traits as a
493 bet-hedging strategy to variable environmental conditions (47, 67). However, such a solitary
494 cell-type may not be sufficient to maintain cooperation in environments that should act
495 favorably for solitary growth (Fig. 3), for example, relatively long nutrient-rich conditions
496 interrupted by brief intervals of starvation. Under such conditions, perturbation be it
497 physiological or genetic that facilitates precocious reversion to solitary state, would be
498 beneficial for individual cells. This notion is supported not only by our growth assay (Fig.
499 3*B*) but also by the fact that there indeed exists a small fraction of cells that are left behind from
500 the rear of a slug that can grow quickly after nutrient recovery (68). In this regard, division
501 of labor in *Dictyostelium,* which less cohesive cells play the altruistic role, has two contrasting
502 end points: 1) they survive as solitary amoeboid cells by being left behind from the slugs (46)
503 and around the basal discs of a culminant (Fig. 2*F*), or 2) they end up in non-viable lower cup
504 cells or basal discs (Figs. 2*B–D*). The social system appears to include a certain proportion of
505 a solitary cell-type in the first place as a bet-hedging strategy, but for those that are socially
506 committed, there is little payoff from quitting cooperation after sensing environment that favors
507 solitary reproduction (Fig. 4). Our study provides a simple explanation for the emergence of
508 collective behavior that is apparently counterintuitive in terms of individual-level fitness.
509
510

511 # Material and Methods

512 Detailed materials and methods can be found in SI text.

513 **Refeeding experiments**

514 Strains expressing cell fate markers were constructed from AX4 cells. To obtain slug-stage
515 cells, vegetative cells were washed with the phosphate buffer (PB), and applied to a 1% PB
516 agar plate and incubated for 18 h. PB containing 20 mM EDTA was applied to the slugs, and
517 the cells were mechanically dissociated by repeated pipetting and passed through a 23 G needle
518 and 40 μm cell strainer. For refeeding, dissociated cells were co-suspended at 2 to 3 × 10^6
519 cells/mL with the concentrated *E. coli* B/r. NF cells were cells suspended in PB immediately

520 after dissociation. The mixed cell suspension at 1 to 2 × 10^6 cells/mL was plated on a glass-
521 bottomed dish (MatTek, Ashland, MA, USA) covered with a thin sheet of 1% PB agar.
522 Confocal fluorescence images were taken using an inverted confocal microscope (Nikon A1+)
523 and Z-slices were obtained using a Ti Z-drive.

524 **Real-time PCR analysis**

525 Dissociated slug cells were suspended in each solution, and shaken at 120 rpm, and harvested
526 at the selected time points. Quantitative PCR amplification (qPCR) was performed using a
527 qPCR thermocycler (ABI7500, Applied Biosystems) with primer pairs and fluorescent beacons
528 (TaqMan probe MGB, Applied Biosystems) (Table S1). The levels of relative gene
529 expression were calculated from the amplification value at the threshold cycle and the relative
530 standard curve for each gene, followed by normalization by *rnlA* amplification as an
531 endogenous control.

532 **Growth assay**

533 Vegetative cells were starved at 2 × 10^6 cells/cm^2. *E. coli* suspension was applied either
534 directly to the slugs or after mechanical dissociation. After 30h incubation, the samples were
535 harvested and washed 2 times to remove the bacteria. Then, 3 × 10^6 cells were transferred
536 into 10 mL of the growth medium and shaken at 120 rpm. The cell number at different times
537 was measured using a hemocytometer.

538 **Statistical analysis**

539 *P*-values from multiple comparisons were adjusted using Holm's method. A generalized
540 linear model (GLM) and analysis of deviance for the fit were performed for the analysis listed
541 in Table S3.

542

543

544 # Author contributions

545 Y.S., M.S., and S.S. designed the research; Y.S. initiated and performed all aspects of the
546 research including data and model analysis; Y.S., N.S., and S.S. contributed new reagents; Y.S.,
547 and S.S. wrote the paper.

548

549

550 # Acknowledgments

551 We thank K. Kaneko for providing critical comments, T. Fujimori, T. Yoshida, and lab
552 members for discussion and technical advice, and A. Nakajima for the microscopy setup. This
553 work was supported by the Platform for Dynamic Approaches to Living System from the
554 Ministry of Education, Culture, Sports, Science, and Technology, Japan to Y.S., M.S., and S.S.;

and by a Grant-in-Aid for Challenging Exploratory Research (Nos. 16K14805) from the Japan Society for the Promotion of Science (JSPS) to Y.S., and M.S. and JSPS Grant-in-Aid 18H04759 and Japan Science and Technology Agency (JST) CREST JPMJCR1923 to S.S..

590 # References

591 1. W. D. Hamilton, The genetical evolution of social behaviour. *J Theor Biol* **7**, 1–52 (1964).

592 2. S. A. Frank, Mutual policing and repression of competition in the evolution of cooperative
593 groups. *Nature* **377**, 520–522 (1995).

594 3. S. A. West, A. S. Griffin, A. Gardner, S. P. Diggle, Social evolution theory for
595 microorganisms. *Nat Rev Microbiol* **4**, 597–607 (2006).

596 4. O. Hallatschek, P. Hersen, S. Ramanathan, D. R. Nelson, Genetic drift at expanding
597 frontiers promotes gene segregation. *Proc Natl Acad Sci USA* **104**, 19926–19930 (2007).

598 5. N. J. Buttery, *et al.*, Structured growth and genetic drift raise relatedness in the social
599 amoeba *Dictyostelium discoideum*. *Biol Letters* **8**, 794–797 (2012).

600 6. S. Smukalla, *et al.*, *FLO1* is a variable green beard gene that drives biofilm-like
601 cooperation in budding yeast. *Cell* **135**, 726–737 (2008).

602 7. H. I. Ho, S. Hirose, A. Kuspa, G. Shaulsky, Kin recognition protects cooperators against
603 cheaters. *Curr Biol* **23**, 1590–1595 (2013).

604 8. G. J. Velicer, L. Kroos, R. E. Lenski, Loss of social behaviors by *Myxococcus xanthus*
605 during evolution in an unstructured habitat. *Proc Natl Acad Sci USA* **95**, 12376–12380
606 (1998).

607 9. B. N. Danforth, Evolution of sociality in a primitively eusocial lineage of bees. *Proc Natl*
608 *Acad Sci USA* **99**, 286–290 (2002).

609 10. T. Y. James, *et al.*, Reconstructing the early evolution of Fungi using a six-gene
610 phylogeny. *Nature* **443**, 818–822 (2006).

611 11. B. E. Schirrmeister, A. Antonelli, H. C. Bagheri, The origin of multicellularity in
612 cyanobacteria. *Bmc Evol Biol* **11**, 45 (2011).

613 12. E. O. Wilson, *The Insect Societies* (Belknap Press, 1971).

614 13. E. O. Wilson, B. Hölldobler, Eusociality: Origin and consequences. *Proc Natl Acad Sci*
615 *USA* **102**, 13367–13371 (2005).

616 14. E. Libby, W. C. Ratcliff, Ratcheting the evolution of multicellularity. *Science* **346**, 426–
617 427 (2014).

618 15. E. Libby, P. L. Conlin, B. Kerr, W. C. Ratcliff, Stabilizing multicellularity through
619 ratcheting. *Phil Trans R Soc B* **371**, 20150444 (2016).

620 16. W. C. Ratcliff, R. F. Denison, M. Borrello, M. Travisano, Experimental evolution of
621 multicellularity. *Proc Natl Acad Sci USA* **109**, 1595–1600 (2012).

622 17. J. J. Bull, E. L. Charnov, On irreversible evolution. *Evolution* **39**, 1149–1155 (1985).

623 18. L. A. Santorelli, *et al.*, Facultative cheater mutants reveal the genetic complexity of
624 cooperation in social amoebae. *Nature* **451**, 1107–1110 (2008).

625 19. A. Khare, *et al.*, Cheater-resistance is not futile. *Nature* **461**, 980–982 (2009).

626 20. P. Manhes, G. J. Velicer, Experimental evolution of selfish policing in social bacteria.
627 *Proc Natl Acad Sci USA* **108**, 8357–8362 (2011).

628 21. M. A. Riley, J. E. Wertz, Bacteriocins: Evolution, Ecology, and Application. *Annu Rev*
629 *Microbiol* **56**, 117–137 (2002).

630 22. N. Danilova, The evolution of immune mechanisms. *J Exp Zool B Mol Dev Evol* **306B**,
631 496–520 (2006).

632 23. J. T. Bonner, *The Cellular Slime Molds* (Princeton University Press, 1967)
633 https:/doi.org/10.1515/9781400876884.

634 24. R. H. Kessin, *Dictyostelium* (Cambridge University Press, 2001)
635 https:/doi.org/10.1017/cbo9780511525315.

636 25. J. E. Strassmann, Y. Zhu, D. C. Queller, Altruism and social cheating in the social amoeba
637 *Dictyostelium discoideum*. *Nature* **408**, 965–967 (2000).

638 26. M. Katoh, G. Chen, E. Roberge, G. Shaulsky, A. Kuspa, Developmental Commitment in
639 *Dictyostelium discoideum*. *Eukaryot Cell* **6**, 2038–2045 (2007).

640 27. K. B. Raper, Pseudoplasmodium formation and organization in *Dictyostelium discoideum*.
641 *J Elisha Mitchell Sci Soc* **56**, 241–282 (1940).

642 28. M. Katoh, *et al.*, An orderly retreat: Dedifferentiation is a regulated process. *Proc Natl*
643 *Acad Sci USA* **101**, 7005–7010 (2004).

644 29. O. M. Gilbert, D. C. Queller, J. E. Strassmann, Discovery of a large clonal patch of a
645 social amoeba: implications for social evolution. *Mol Ecol* **18**, 1273–1281 (2009).

646 30. G. Chen, O. Zhuchenko, A. Kuspa, Immune-like Phagocyte Activity in the Social
647 Amoeba. *Science* **317**, 678–681 (2007).

648 31. P. C. Newell, M. Longlands, M. Sussman, Control of enzyme synthesis by cellular
649 interaction during development of the cellular slime mold *Dictyostelium discoideum*. *J Mol*
650 *Biol* **58**, 541–554 (1971).

651 32. H. Deichsel, *et al.*, Green fluorescent proteins with short half-lives as reporters in
652 *Dictyostelium discoideum*. *Dev Genes Evol* **209**, 63–68 (1999).

653 33. C. H. Siu, B. D. Roches, T. Y. Lam, Involvement of a cell-surface glycoprotein in the
654 cell-sorting process of *Dictyostelium discoideum*. *Proc Natl Acad Sci USA* **80**, 6596–6600
655 (1983).

656 34. C. H. Siu, T. J. C. Harris, J. Wang, E. Wong, Regulation of cell–cell adhesion during
657 *Dictyostelium* development. *Semin Cell Dev Biol* **15**, 633–641 (2004).

658 35. T. E. Crowley, W. Nellen, R. H. Gomer, R. A. Firtel, Phenocopy of discoidin I-minus
659 mutants by antisense transformation in *Dictyostelium*. *Cell* **43**, 633–641 (1985).

660 36. E. Bastounis, B. Álvarez-González, J. C. del Álamo, J. C. Lasheras, R. A. Firtel,
661 Cooperative cell motility during tandem locomotion of amoeboid cells. *Mol Biol Cell* **27**,
662 1262–1271 (2016).

663 37. T. Fujimori, A. Nakajima, N. Shimada, S. Sawai, Tissue self-organization based on
664 collective cell migration by contact activation of locomotion and chemotaxis. *Proc Natl Acad*
665 *Sci USA* **116**, 4291–4296 (2019).

666 38. M. S. Steinberg, M. Takeichi, Experimental specification of cell sorting, tissue spreading,
667 and specific spatial patterning by quantitative differences in cadherin expression. *Proc Natl*
668 *Acad Sci USA* **91**, 206–209 (1994).

39. K. Parkinson, *et al.*, Regulation of Rap1 activity is required for differential adhesion, cell-type patterning and morphogenesis in *Dictyostelium*. *J Cell Sci* **122**, 335–344 (2009).

40. R. E. Finney, L. H. Mitchell, D. R. Soll, B. A. Murray, W. F. Loomis, Loss and resynthesis of a developmentally regulated membrane protein (gp80) during dedifferentiation and redifferentiation in *Dictyostelium*. *Dev Biol* **98**, 502–509 (1983).

41. T. Y. Lam, G. Pickering, J. Geltosky, C. H. Siu, Differential cell cohesiveness expressed by prespore and prestalk cells of *Dictyostelium discoideum*. *Differentiation* **20**, 22–28 (1981).

42. W. F. Whittingham, K. B. Raper, Non-viability of stalk cells in *Dictyostelium*. *Proc Natl Acad Sci USA* **46**, 642–649 (1960).

43. B. J. Harrington, K. B. Raper, Use of a fluorescent brightener to demonstrate cellulose in the cellular slime molds. *Appl Microbiol* **16**, 106–113 (1968).

44. K. Jermyn, D. Traynor, J. Williams, The initiation of basal disc formation in *Dictyostelium discoideum* is an early event in culmination. *Development* **122**, 753–760 (1996).

45. D. J. Watts, T. E. Treffry, Culmination in the slime mould *Dictyostelium discoideum* studied with a scanning electron microscope. *J Embryol Exp Morphol* **35**, 323–333 (1976).

46. J. Sternfeld, A study of PstB cells during *Dictyostelium* migration and culmination reveals a unidirectional cell type conversion process. *Roux's Arch Dev Biol* **201**, 354–363 (1992).

47. D. Dubravcic, M. van Baalen, C. Nizak, An evolutionarily significant unicellular strategy in response to starvation in *Dictyostelium* social amoebae. *F1000research* **3**, 133 (2014).

48. S. A. H. Geritz, É. Kisdi, G. Meszéna, J. A. J. Metz, Evolutionarily singular strategies and the adaptive growth and branching of the evolutionary tree. *Evol Ecol* **12**, 35–57 (1998).

49. U. Dieckmann, R. Ferrière, "Adaptive Dynamics and Evolving Biodiversity" in *Evolutionary Conservation Biology*, R. Ferrière, U. Dieckmann, D. Couvet, Eds. (Cambridge University Press, 2004), pp. 188–224.

50. J. M. Smith, *Evolution and the theory of games* (Cambridge University Press, 1982).

695 51. I. Eshel, Evolutionary and continuous stability. *J Theor Biol* **103**, 99–111 (1983).

696 52. T. Abe, A. Early, F. Siegert, C. Weijer, J. Williams, Patterns of cell movement within the
697 *Dictyostelium* slug revealed by cell type-specific, surface labeling of living cells. *Cell* **77**,
698 687–699 (1994).

699 53. M. E. Hochberg, D. J. Rankin, M. Taborsky, The coevolution of cooperation and dispersal
700 in social groups and its implications for the emergence of multicellularity. *Bmc Evol Biol* **8**,
701 238 (2008).

702 54. C. N. Jack, *et al.*, Migration in the social stage of *Dictyostelium discoideum* amoebae
703 impacts competition. *Peerj* **3**, e1352 (2015).

704 55. J. M. Nichols, *et al.*, Cell and molecular transitions during efficient dedifferentiation.
705 *eLife* **9**, e55435 (2020).

706 56. R. Lande, Expected time for random genetic drift of a population between stable
707 phenotypic states. *Proceedings of the National Academy of Sciences of the United States of*
708 *America* **82**, 7641–7645 (1985).

709 57. Y. Iwasa, F. Michor, M. A. Nowak, Stochastic tunnels in evolutionary dynamics. *Genetics*
710 **166**, 1571–1579 (2004).

711 58. J. Sternfeld, The anterior-like cells in *Dictyostelium* are required for the elevation of the
712 spores during culmination. *Dev Genes Evol* **208**, 487–494 (1998).

713 59. J. Sternfeld, C. N. David, Cell Sorting daring Pattern Formation in *Dictyostelium*.
714 *Differentiation* **20**, 10–21 (1981).

715 60. D. Dormann, F. Siegert, C. J. Weijer, Analysis of cell movement during the culmination
716 phase of *Dictyostelium* development. *Development* **122**, 761–769 (1996).

717 61. T. Saito, A. Kato, R. R. Kay, DIF-1 induces the basal disc of the *Dictyostelium* fruiting
718 body. *Dev Biol* **317**, 444–453 (2008).

719 62. G. Bichler, C. J. Weijer, A *Dictyostelium* anterior-like cell mutant reveals sequential steps
720 in the prespore prestalk differentiation pathway. *Development* **120**, 2857–2868 (1994).

63. J. M. Smith, E. Szathmáry, *The Major Transitions in Evolution* (Oxford University Press, 1995).

64. R. E. Michod, D. Roze, "Cooperation and conflict in the evolution of individuality. III. Transitions in the unit of fitness" in Mathematical and Computational Biology: Computational Morphogenesis, Hierarchical Complexity, and Digital Evolution., C. L. Nehaniv, Ed. (American Mathematical Society, 1999), pp. 47–92.

65. C. Hauert, S. D. Monte, J. Hofbauer, K. Sigmund, Replicator dynamics for optional public good games. *J Theor Biol* **218**, 187–194 (2002).

66. T. Garcia, G. Doulcier, S. D. Monte, The evolution of adhesiveness as a social adaptation. *eLife* **4**, e08595 (2015).

67. C. E. Tarnita, A. Washburne, R. Martinez-Garcia, A. E. Sgro, S. A. Levin, Fitness tradeoffs between spores and nonaggregating cells can explain the coexistence of diverse genotypes in cellular slime molds. *Proc Natl Acad Sci USA* **112**, 2776–2781 (2015).

68. J. J. Kuzdzal-Fick, K. R. Foster, D. C. Queller, J. E. Strassmann, Exploiting new terrain: an advantage to sociality in the slime mold *Dictyostelium discoideum*. *Behav Ecol* **18**, 433–437 (2007).

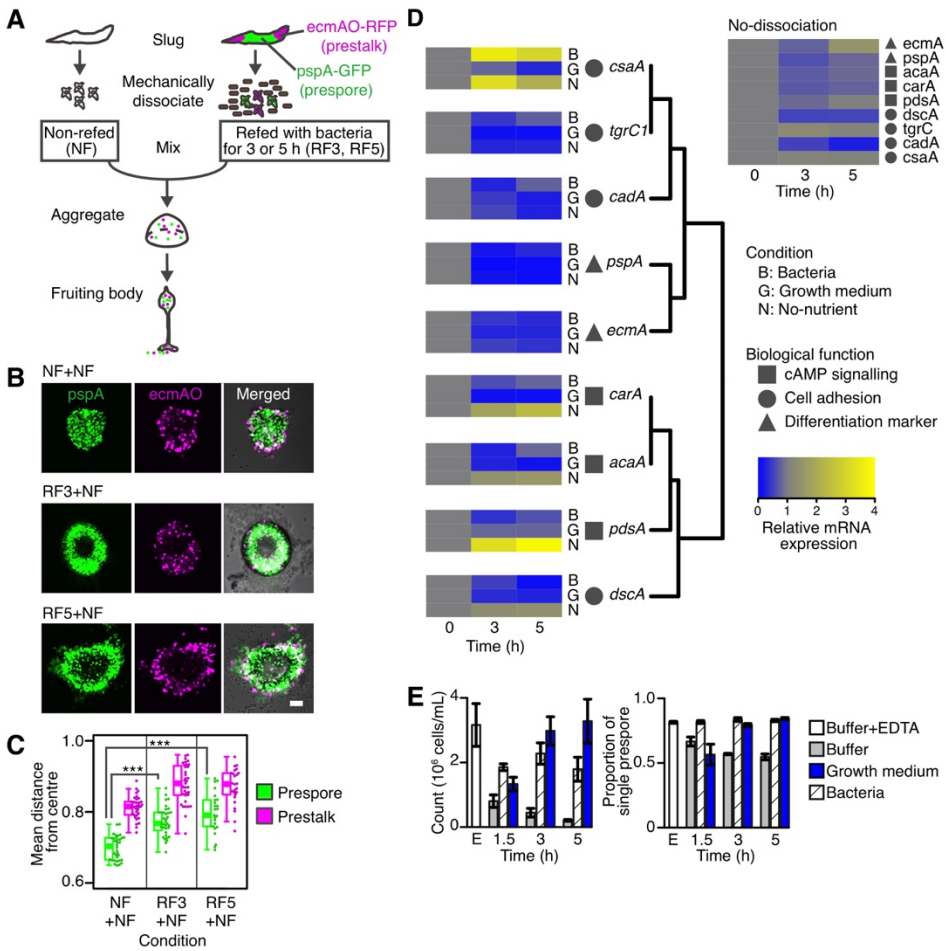

750

751 **Figure 1 Prestalk-like positioning and cell-state of refed cells.** (*A*) A schematic of
752 refeeding and reaggregation of a cell mixture. Dissociated cells shaken with *E. coli* for 3 or 5
753 h (Refed: RF3, RF5), washed and mixed with non-refed cells (Non-refed: NF) for development
754 on agar. RF cells harbored prestalk (ecmAO-RFP, magenta) and prespore (pspA-GFP, green)
755 markers. NF cells were the parental wild-type strain (AX4). (*B*) Representative images of
756 mixed aggregates 1.5–2 h after plating (pspA: GFP-channel, ecmAO: RFP-channel, Merged:
757 bright-field (grayscale) and fluorescence images). 'NF+NF': NF cells with the cell-type
758 reporter mixed with NF cells without the cell-type reporter as a control condition. 'RF3+NF'
759 and 'RF5+NF': Mixture of NF cells and RF3 or RF5 cells, respectively at RF:NF = 15:85 ratio.
760 A scale bar = 50 µm. (*C*) Normalized mean distance between the aggregate center and cells
761 of prestalk- or prespore-origin. The sample size N (biological replicate, aggregates): NF+NF
762 = (4, 34), RF3+NF = (4, 35), RF5+NF = (3, 25). Circles: Values for individual aggregates,
763 lines inside of box plots: The median values. *** $P < 0.0001$ by *t* test. (*D-E*) Cell-state
764 change incurred by the nutrient and dissociation. (*D*) qRT-PCR analysis. Gene expression
765 levels of dissociated cells in bacterial suspension 'B', growth medium 'G', non-nutrient buffer
766 'N' (left panel). Unperturbed slugs 18 h into starvation onward ('No-dissociation': Upper

767 right panel). Gene expression levels were normalized by the 0 h point. Gene targets were
768 clustered hierarchically. The sample size N = 3 are biological replicates. (*E*) Differences in
769 cell cohesiveness between RF and NF cells. Number of single cells within a sample in
770 different solutions (left panel). Proportion of single prespore cells in the total single cells
771 within a sample (right panel). 'E': Cells in the phosphate buffer containing EDTA
772 (Buffer+EDTA) as a control (most cells were in a single state). The number (1.5, 3, and 5)
773 indicates hours shaken in suspensions. The sample size N =3 are biological replicates, with
774 380–5966 cells per condition. Error bars are standard error.
775
776
777
778
779
780
781
782
783
784
785
786
787
788
789
790
791

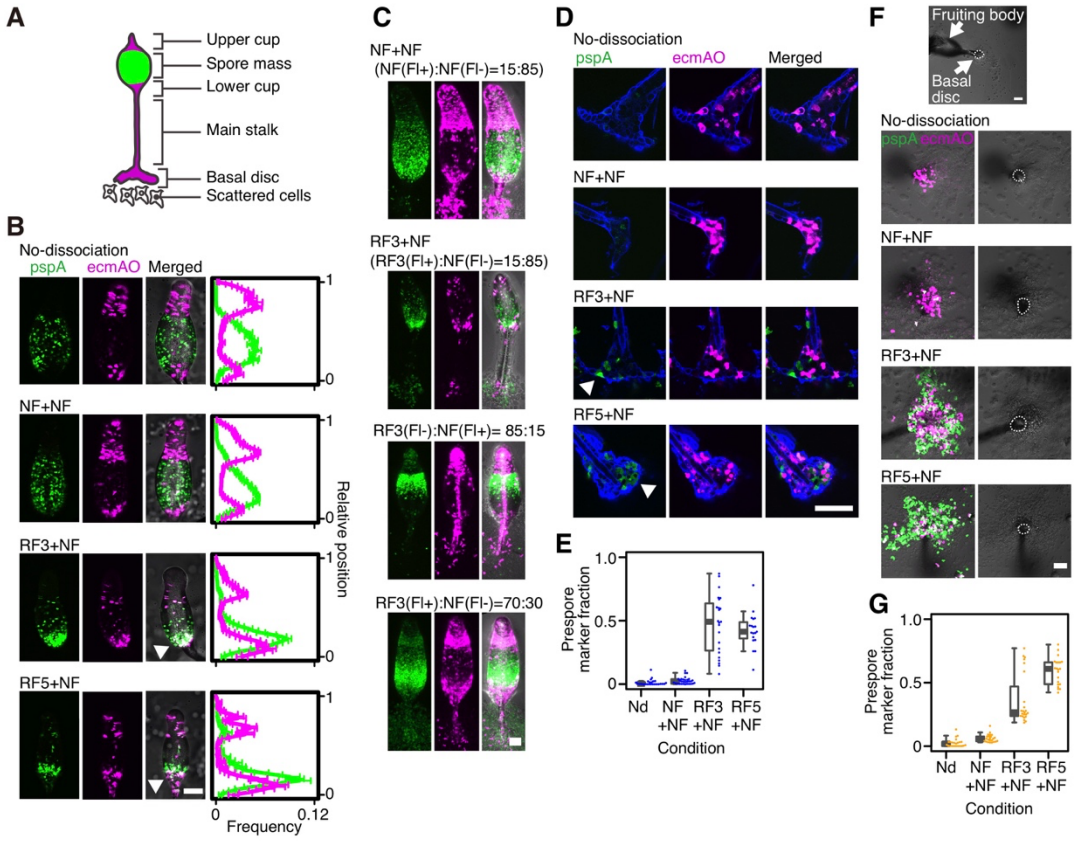

Figure 2 Refeeding redirects cells to the role of prestalk subtype. (*A*) A schematic illustration of the fruiting body. (*B*) Snapshots of the upper region of early fruiting bodies (left). Frequency of prestalk (magenta line) and prespore (green) marker-positive pixels along the anterior-posterior axis (right). No-dissociation (Nd): A fruiting body formed by unperturbed cells. In RF3+NF and RF5+NF, RF cells were found exclusively at the lower cup (arrow heads). The sample size N (biological replicate, fruiting body number): N: Nd = (2, 14), NF+NF = (3, 24), RF3+NF = (3, 20), RF5+NF = (3, 13). For abbreviations, see also Fig.1. (*C*) Early fruiting bodies consisted of different ratios of RF3 and NF cells. Fl+, Fl-: with/without cell-type markers, respectively. (*D*) Fluorescent images of the basal disc. Images of stalk cellulose staining (blue, calcofluor white) were merged with fluorescence images (pspA, ecmAO). Note RF cells of prespore origin are found in the basal disc (RF3+NF and RF5+NF) (arrow heads). (*E*) The ratio of prespore marker-positive to prestalk region in the basal disc. N: Nd = (3, 26), NF+NF = (3, 30), RF3+NF = (3, 23), RF5+NF = (3, 19). (*F*) Representative images of the basal region of fruiting bodies. Note isolated RF cells (fluorescent cells, left panel) scattered around the basal discs (white circles, right panel) in RF3+NF and RF5+NF. (*G*) The ratio of prespore marker-positive region to prestalk region in the scattered cells. N: Nd = (3, 23), NF+NF = (3, 23), RF3+NF = (3, 23), RF5+NF = (3, 21). All scale bars = 50 μm. Error bars: Standard error.

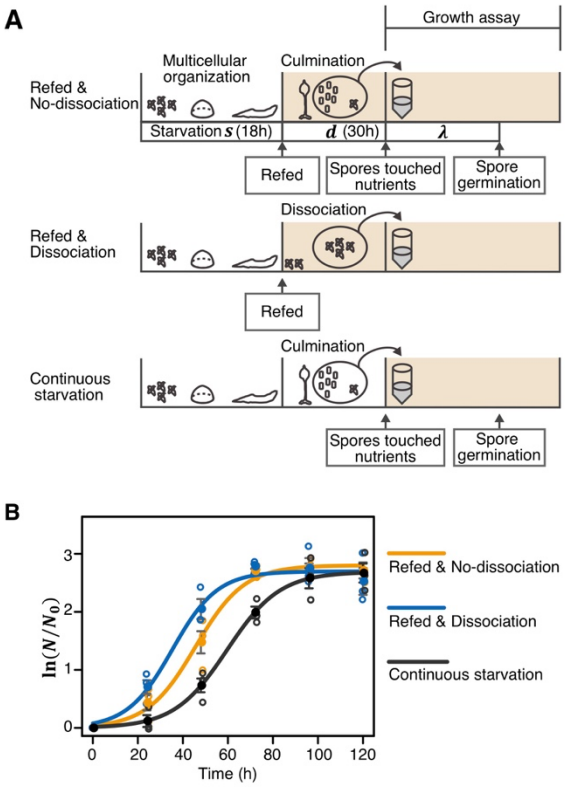

Figure 3 The social commitment imposes growth cost under nutrient recovery. (*A*) The schematic of the growth assay. Cells in the slug stage (s =18 h) are exposed to nutrient recovery. After 30h incubation (d) for the fruiting body maturation, cells were transferred into the growth medium ('Growth assay'). Under social commitment ('Refed & No-dissociation' and 'Continuous starvation'), cells ignore nutrient and develop into a fruiting body. Thus, cells restart growing after spore germination with the lag time λ. Without social commitment ('Refed & Dissociation'), cells quickly restart growing immediately after refeeding. (*B*) Growth curve assay. 'Refed & No-dissociation' (orange): A growth curve of cells from the non-dissociated refed slugs, 'Refed & Dissociation' (blue): Cells from refed slugs that were dissociated to release cells from social commitment, 'Continuous starvation' (black): Uninterrupted development under continued starvation. $\ln(N/N_0)$: Logarithm of relative population size that was normalized by the initial cell number. The error bars: Relative error. Circles: Individual values from three biological replicates. Regrowth of refed cells from non-dissociated slugs were significantly delayed compared to that of dissociated slugs (GLM, $P <$ 0.003).

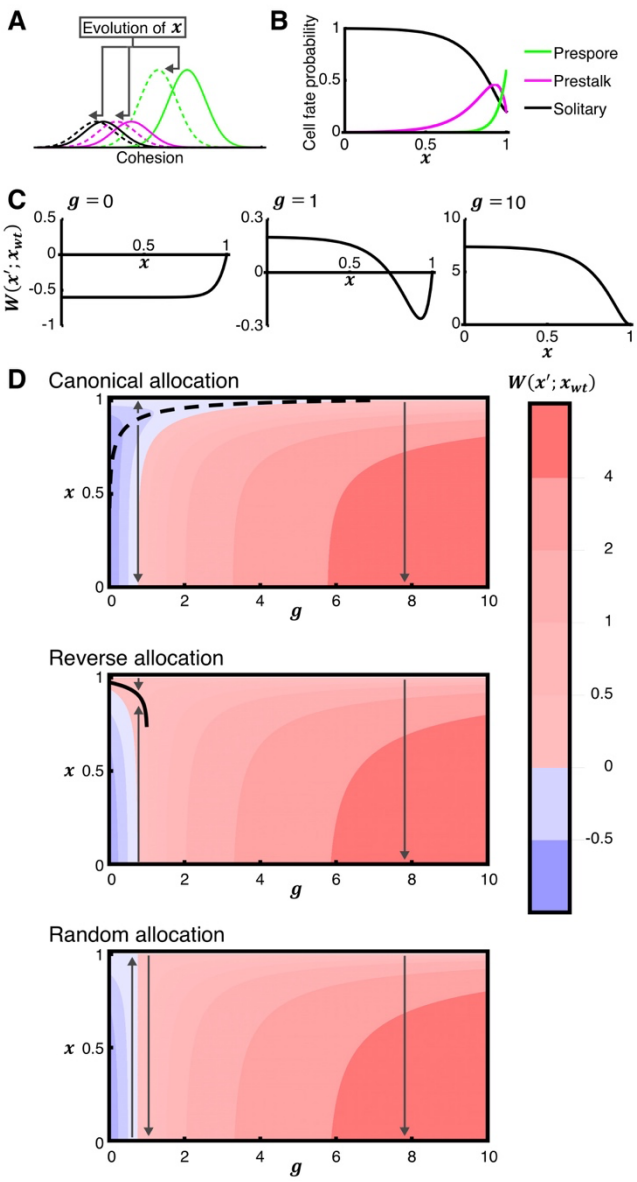

Figure 4 Social commitment in *Dictyostelium* is an evolutionarily stable strategy. (*A*) A intuitive explanation of cell fate transitions via evolution of trait x. The trait x $(0 \leq x \leq 1)$ decides the cell-cell association level, which generally controls most of cohesion proteins as a 'master regulator' ($x = 1$: full social commission, $x = 0$: a solitary state, complete degradation of cohesion proteins). The solid lines indicate cohesion distributions of prespore (green), prestalk (magenta), and solitary cells (black) in the cell population. The evolution of reduced x can be illustrated as distribution shifts (dotted line). After the evolution, prespore cells (dotted green line) will exhibit reduced cohesion similar to original prestalk and solitary cells (solid magenta and black lines). From our experiments (Figs.1 and 2), cells are assumed to play a cell-fate role as determined by their own cohesivity. (*B*) Evolution of x and its link to the cell fate probability (Eq. **1**) for a spore (green), stalk (magenta), solitary cell (black), respectively. (*C*) The invasion fitness of the solitary reversion mutant within the wild-type

population $W(x'; x_{wt})$, where the wild-type trait is $x_{wt} = 1$. g is the additional weight for the solitary fitness as defined by nutrient availability. Note that the fitness function has a valley in the intermediate nutrient condition ($g = 1$) suggesting that the mutant cannot evolve when the evolution starts from the vicinity of $x = 1$. (*D*) Evolutionary directions and equilibrium under various environmental conditions. Black lines indicate analytical predictions for the singular point x^* (dotted line: Evolutionary repellor, solid line: Evolutionary attractor). Allows indicates the direction of selection. The red and blue colors indicate invasion fitness of the mutant interacts with the wild-type cell with $x_{wt} = 1$.

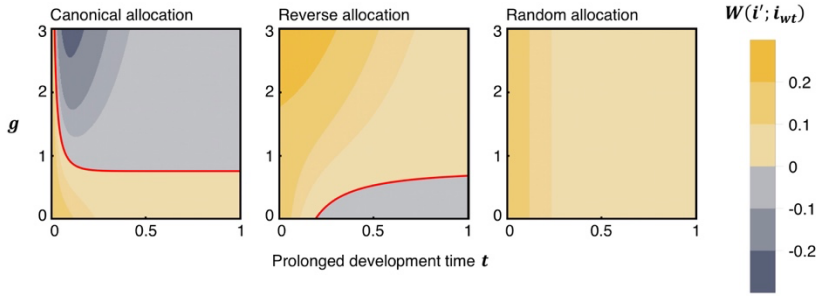

Figure 5 Division of labor in *Dictyostelium* effectively reduces cheating advantage. Evolutionary trait i describes additional spore investment, i_{wt}: The wild-type cell trait, i': The cheating mutant trait ($i_{wt} < i'$). $W(i'; i_{wt})$: Invasion fitness of the cheating mutant within the wild-type population. t: Prolonged development time from the slug stage. Red lines indicate the analytical predictions whether the cheater invades the wild-type population. The cheater can invade under the conditions below the red line in canonical allocation system, and above the line in reverse allocation system. In random allocation, cheating always evolved. Initial cell fate probability of the mutant being prespore: 0.8, prestalk: 0, solitary cell: 0.2, that of the wild-type strain being prespore: 0.6, prestalk: 0.2, solitary cell: 0.2 are shown.